We are IntechOpen, the world's leading publisher of Open Access books Built by scientists, for scientists

4,800
Open access books available

122,000
International authors and editors

135M
Downloads

Our authors are among the

154
Countries delivered to

TOP 1%
most cited scientists

12.2%
Contributors from top 500 universities

CLARIVATE ANALYTICS BOOK CITATION INDEX INDEXED

WEB OF SCIENCE™

Selection of our books indexed in the Book Citation Index in Web of Science™ Core Collection (BKCI)

Interested in publishing with us?
Contact book.department@intechopen.com

Numbers displayed above are based on latest data collected.
For more information visit www.intechopen.com

7

Origin of HED Meteorites from the Spalling of Mercury – Implications for the Formation and Composition of the Inner Planets

Anne M. Hofmeister and Robert E. Criss
Department of Earth and Planetary Sciences,
Washington University in St Louis, MO,
USA

1. Introduction

The bulk chemical composition of the Earth is poorly constrained because samples are limited to only the outer 10% of its radius. Meteorite data are used to represent the huge zones that we cannot sample, but for this approach to provide a realistic model of the Earth, we need to know where various meteorites originated and what processing they underwent. Currently popular models of the Solar System presume that the Sun formed first, followed by assembly of the planets from mineral dust in a disk that condensed locally from hot gas (e.g., Boss, 1998). More recent findings that comets are mixtures of phases formed at high and low temperature (Zolensky et al., 2006) came as a great surprise to planetary scientists because this contraindicates the existence of a condensation gradient as proposed by Lewis (1974). The alternative to dust condensation around a pre-formed Sun is a nebula containing dust inherited from older generations of stars. Meteorites possess small amounts of isotopically distinctive pre-solar material, proving that the nebula included some dust that predates our Sun (e.g., Bernatowicz & Zinner, 1997). Recent detection of silicate dust in molecular clouds (van Breeman et al., 2011), which are loci of star formation, suggests that pre-solar dust was abundant. Disk models also have problems conserving angular momentum (Armitage, 2011) and fail to explain the first order characteristics of the Solar System (upright axial spin and nearly circular orbits). Thus, independent evidence points to formation of planets and Sun simultaneously from a 3-dimensional dusty nebula (Hofmeister & Criss, 2012), in which case, virtually all meteoritic material has been processed. What represents the bulk Earth?

It is generally accepted that chondritic meteorites are very primitive material, and bulk compositions of the silicate Earth have been derived from various averages. Models based on enstatite chondrites (Javoy, 1995; Lodders, 2000), which have Earth-like oxygen isotopes and Fe-metal content, agree with heat flux measurements (Hofmeister & Criss, 2005). Newly measured flux of neutrinos from within the Earth (Gando et al., 2011) support the enstatite chondrite model. However, because even the most primitive meteorites show some evidence of alteration and are comprised of non-equilibrium assemblages (e.g., Brearley & Jones, 1998), bulk compositions so derived are estimates, not exact representations of the Earth. Hence, it is worthwhile to consider alternative means of inferring bulk composition.

The present paper considers how more processed meteorites (the differentiated achondrites) may be related to the Earth. We demonstrate that the largest class of achondrites (the HEDs) has been wrongly assigned to an asteroidal parent body: a planet is required. The likely source is evolving Mercury, which suffered severe impacts that ejected the majority of its mantle to space (Section 1.2). This connection permits us to decipher information about the Earth during core formation, a very early and important step in its history which is not documented in terrestrial samples, and to estimate bulk planetary composition.

1.1 Problems in assigning HED meteorites to the asteroid Vesta

Many different classes of achondrites are recognized, but most of these classes contain few meteorites (e.g., Mittlefehldt et al., 1998, summarized in Table 1). The largest single class of achondrites, the HEDs (= howardite, eucrite, and diogenite) is a distinctive petrographic family whose affinity has been confirmed by oxygen isotopes (e.g., Taylor et al., 1965). Eucrites are similar to pigeonite-plagioclase basalts and basaltic cumulates, while diogenites are similar to orthopyroxenites, and howardites are brecciated mixtures of these two types (e.g., Dymek et al., 1976; Shearer et al., 1997). It is further recognized that mesosiderites, pallasites, and IIIAB iron meteorites are geochemically similar to each other and to HEDs (e.g., Duke & Silver, 1967; Clayton & Mayeda, 1996). Section 5 provides further discussion.

Main type	Description	Type	Mineralogy	ρ, g cm^{-3}	Number	Total kg
Chondrites	unmelted stones*	ordinary	pyroxene, olivine	3.3	36326	43000
		carbonaceous	hydrated, C	2.1-3.5	1385	3281†
		enstatite	~$MgSiO_3$, albite	3.6	506	850
Achondrites	melted stones	HEDs‡	basaltic, see text	2.9-3.3	1033‡	1250‡
		Martian	pigeonite, olivine	3.2	99	100
		Lunar	anorthite, basalt	2.7, 3.8	146	60
		other§	as above, fassaite	~3	576§	4700§
Stony- irons	Metal+ silicates	mesosiderites‡	HED minerals	4.2	170‡	6300‡
		pallasites‡	olivine	4.8	89‡	13100‡
Irons	Fe with<20% Ni	non-magmatic	most have low Ni	7.5	280	150000
		magmatic IIIAB‡	most have low Ni	7.5	288‡	136000‡
		other magmatic	variable Ni	7.5	485	164000

* Most contain chondrules (spheres of once melted material, typically olivine+pyroxene+feldspar rim or of forsterite+enstatite+Fe^0), calcium-aluminum-rich inclusions, and/or pre-solar grains.
† Virtually all carbonaceous chondrite mass is in the Allende meteorite (3000 kg).
‡ Part of the HED family, sensu lato.
§ Of the remaining achondrites, 298 are C-rich ureilites but 67 aubrites (related to enstatite chondrites) have 4300 kg of the mass. Brachinites and angrites have chemical affinities to HEDs (Section 5).

Table 1. Summary of meteorite types with simple descriptions. Density from Britt and Consolmagno (2003). Number and mass from *The Meteoritical Bulletin* database (www.lpi.usra.edu/meteor/metbull.php, accessed 9/26/2011).

Sourcing the HEDs to the 3rd largest asteroid, Vesta, is based on spectral comparisons (e.g., Gaffey, 1997). Slight variations in spectra across its surface were interpreted as differing proportions of pigeonite to other phases. Detection of a basaltic mineral was taken as evidence that the asteroid had differentiated, and thus has a core (e.g., Ruzika et al., 1997).

Attribution of HED meteorites to Vesta and a few spectrally similar asteroids, despite weak evidence for orthopyroxenes or olivine (e.g., Burbine et al., 2001), sets the view that this tiny object is a major parent body. Spectral variations do not require differentiation: 1) dust on the surface could be non-uniform in grain-size, distribution, or mineral proportions, 2) Vesta could be a remnant from a larger body, or 3) Vesta could be a conglomerate, as are many meteorites. Section 2 shows that Vesta is too small to sort phases by density in its own gravitational field. Section 4 shows that grain-size variations explain Vesta's spectra.

The Vesta hypothesis is counter-evidenced by the abundance of HEDs, which outnumber all other achondrites combined (Table I). Assignment of the HEDs to Vesta further requires a few asteroids provide IIIAB irons, and most mesosiderites and pallasites, which constitute a huge proportion of the collection (Table I). It is far more likely that Vesta and similar asteroids are cousin fragments of a much larger parent body.

Dynamical arguments that were set forth against proposals of Mars as the source of SNC meteorites (e.g., Vickery & Melosh, 1983) were refuted by subsequent isotopic and chemical evidence (summarized by Grady, 2006). Recognition of lunar and Martian meteorites, coupled with Mercury being of intermediate size to these parent bodies led Love & Kiel (1995) to suggest that some Mercurian samples may reside in available collections. Although impact calculations have been extensively revised to explain the existence of lunar and Martian meteorites, the view is nevertheless still held that dynamics forbid Mercury as a meteorite source (e.g., Melosh & Tonks, 1993). Clearly, dynamical arguments can neither prove nor preclude planetary ejection, let alone establish transport. Problems with such modeling are covered in Sections 1.2 and 3.

1.1.1 Is Vesta a mesosiderite? Was Vesta highly impacted?

Low orbital eccentricity of ~0.09 for Vesta and Ceres, compared to an average of 0.26 for 25 large asteroids which is similar to those of Pallas and Juno (http://nssc.gsfc.an.gov), indicates that Vesta was not more heavily impacted. We propose that Vesta is a mesosiderite with ~20% iron, based on its density of 3.9 g cm^{-3}, and spectra (Section 4), and represents below of 1% of the mass ejected from Mercury. High iron content provides material strength. The lumpy shape resembles that of iron-rich meteorites.

1.2 Is early Mercury the source of HEDs and related meteorites?

Mercury's unique characteristics are its high orbital eccentricity (0.2056 compared to 0.0067-0.094 for the other seven planets), the large size of its Fe core compared to its mantle, and its similarity to the Moon, with craters upon craters, ejecta, impact basins, and smooth plains that are probably volcanic (e.g., Spudis & Guest, 1988). Delivery of immense kinetic energy in an impact is evidenced by the Caloris basin, and its antipodal structure.

Various hypotheses attempt to explain Mercury's special characteristics. Attribution of Mercury's Fe rich composition to high-temperature nebular condensates being located near the Sun (Lewis, 1974) cannot be the cause because condensation temperatures of Fe^0 and Mg_2SiO_4 (forsterite) only differ by a few degrees (Lodders, 2003) which precludes their sorting during condensation. Attribution of Fe-enrichment to vaporization of its surface (Cameron et al., 1988) does not address high orbital eccentricity and requires excessively

high surface temperatures. It is difficult to reconcile the topography with vaporization. Loss of Mercury's mantle through catastrophic fragmentation following many giant impacts, in which most of the material was reassembled while Mercury's orbit ranged dramatically, including beyond the Earth (Wetherill, 1988) has problems as regards orbital excursions, and incorrectly assumes that the impactor plus Mercury constituted a bound state, see Section 3.

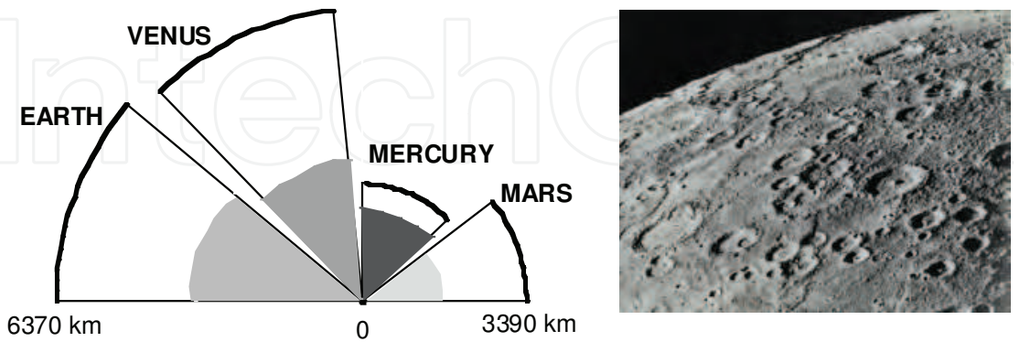

Fig. 1. Mercury's internal structure and surface features. Left = comparison of the terrestrial planets to scale. Surfaces = heavy lines. Metal cores = shaded sections. Data from Lodders & Fegely (1998). Right = photo of a limb of Mercury taken by the Mariner spacecraft. The lower edge shows about 560 km across. From http://history.nasa.gov/EP-177/ch2-2-2.html.

Hofmeister and Criss (2012) recently proposed a different history for Mercury, whereby repeated impacts stripped away the mantle through the late heavy bombardment (LHB) that occurred up to 800 Ma after formation (Gomes et al., 2005). Given the physical characteristics of Mercury, its proximity to the gravitational focus of the Solar System (the Sun), and events like the LHB we propose that the spallation of Mercury before core formation was complete provided HEDs, pallasites, mesosiderites, irons, and others. Minimal addition of kinetic energy is needed to promote ejecta to distant orbits (Section 3). We conclude that the asteroid belt is a junkyard of debris that originated from diverse regions of the Solar System over its history, particularly small bodies (e.g., various moons, Mars, and Mercury as it evolved) and outer Solar System primitive material drawn in, e.g., during the LHB. Oxygen isotope data implicate early Mercury as the parent body of the HEDs (Section 5) and lead to bulk chemical compositions for Earth and its core (Section 6).

2. Did Vesta differentiate under its own gravity?

This section compares characteristics of Vesta to those of bodies with known cores. The observed trends are explained using Stokes' law and stability arguments.

2.1 Limitation of known cores to round, large bodies

Small planets are cold relative to large, due to their high surface area to volume ratio, which provides for greater radiative cooling to space, and shorter distances over which internal heat diffuses. Hence, their potential for differentiation via convection and gravitational segregation is limited. Mass fractions of planetary cores depend on planetary radius (Fig. 2a). Trends of the rocky bodies suggest that a minimum radius of ~1200 km is required to form a core. Considering icy and rocky bodies for which the moment of inertia is known, differentiation is also associated with a minimum surface gravitational acceleration (g) of

~1.2 ms^{-2} (Fig. 2b). The trends show that an object must have a mass in excess of ~10^{22} kg to have a metallic core, which is greater than the mass of the entire asteroid belt.

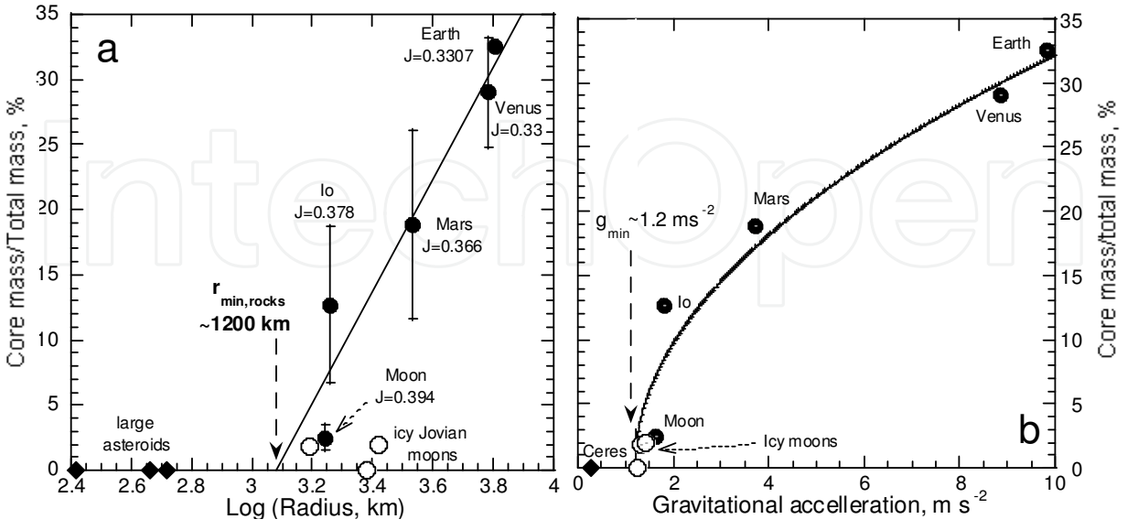

Fig. 2. Dependence of core size, expressed as the ratio of core mass to total planetary mass, on (a) the logarithm of the surface radius and (b) the surface gravitational acceleration. Diamonds = asteroids. Dots (with error bars) = rocky moons. Open circles = icy moons with highly uncertain core sizes. Mercury was not included in the linear regression, although the x-intercept of the fits would change little if it were. Measured moments of inertia ($J=I/Mr^2$ where r is radius and M is total mass) are indicated. Bodies with cores have $J<0.4$, which is the value for a sphere of constant density. Dashed vertical arrows emphasize minimum values needed for core formation. Data from Lodders & Fegley (1998).

2.2 A minimum planetary size is required for gravitational settling

Core size correlates with both g and R (Fig. 2) because the latter are related through:

$$g = 4\pi\rho G R/3 \quad (1)$$

where G is the gravitational constant, and ρ is the mean density. Forming a planetary core involves sorting of different density phases in a gravitational field. We therefore focus our discussion on gravitational acceleration. Because iron and silicate melts are immiscible (e.g., Goodrich and Bird, 1985) and density of liquids and crystals generally correlate, core formation can be viewed as sinking of Fe^0 particles or blobs within a silicate "fluid" in the hot interior of the planet. Settling is described in terms of a Stokes (terminal) velocity:

$$v = g\Delta\rho d^2/(18\eta), \quad (2)$$

where η is dynamic viscosity of the "fluid," d is particle diameter, and Δρ is the density difference between the particle and the fluid. The percentage difference between $\rho_{silicate}$ and ρ_{ice} being similar to that of ρ_{Fe} and $\rho_{silicate}$ and η being related to the density (compression) explains why one trend in surface g exists for bodies with different compositions (Fig. 2b).

The core grows at a rate comparable to Stokes' velocity. Large planets with large g remain hot longer, forming proportionately larger cores (Fig. 2b). For bodies with g exceeding ~2 $m{\cdot}s^{-2}$, core size directly depends on g, as indicted by Eq. 2. Because large planets retain more heat than small, viscosity decreases as planet size increases which makes the dependence of v on g weaker than linear. However, Eq. 2 assumes that particles sink and reach a terminal velocity within the static fluid, but does not describe whether sinking is possible. Figure 2 demonstrates that a minimum g is needed for coherent, downward motions.

Asteroids are too small to possess cores. It is immaterial whether asteroidal bodies are mixtures of iron and silicate or of silicate and ice, given similar density contrasts. Because the density contrast among various silicate mineral pairs are an order of magnitude smaller, asteroids could not have sorted olivine from plagioclase. Our conclusion that Vesta and all other asteroids could not differentiate due to internal gravitational sorting does not preclude these being differentiated material. Rather, our analysis shows that the differentiation occurred within a larger body with sufficient mass to permit density sorting.

3. Derivation of achondrites from the inner Solar System

Derivation of meteorites from Mars has been demonstrated (summarized by Grady, 2000). Mercury has g = 3.70 $m{\cdot}s^{-2}$, close to that of Mars (3.71 $m{\cdot}s^{-2}$) and an escape velocity of 4.3 $km{\cdot}s^{-1}$, low compared to Mars (5 $km{\cdot}s^{-1}$). Together these characteristics show that ejection of material from Mercury is not merely possible, but expected. Hence, objections to Mercury as a parent body rest on the notion that transport of material outward from the innermost Solar System is prohibited due to the huge gravitational influence of the Sun (e.g., Melosh & Tonks, 1993; summarized by Love & Kiel, 1995). Such difficulties have been overstated. As discussed below in general terms, classical mechanics indicates transport is feasible.

3.1 Dynamical constraints

Calculations concerning ejection of objects from planetary bodies and the consequent orbits are a variant of the three-body problem of classical mechanics. A system of three or more masses, moving under their mutual gravitational forces, cannot be solved in any general way (e.g., Goldstein, 1950; Symon, 1971). For example, the three-body problem cannot be reduced to three one-body problems. Very few special solutions exist: 1) the restricted three-body problem can be solved, wherein one mass is small and does not perturb the motions of the other two large masses (e.g., the trajectory of a rocket from Earth to the Moon); 2) motions of the planets can be accurately calculated, which represent a numerical solution obtained from specified initial conditions that holds over some period of time; and 3) a particular solution exists for three-bodies orbiting about the center of mass (discovered by Lagrange). Dynamical studies of ejection of material from planets, and the resultant trajectories, are neither general nor particular solutions to the n-body problem, but are numerical results predicated on various assumptions, whether implicitly or explicitly stated. Hence, the fate of an impact can only be deduced in general terms from simple approaches.

3.2 Outward transport of material ejected during collisions

The total kinetic and potential energy of a particle in an elliptical orbit depends on the semi-major radius but not on the eccentricity (e), semi-minor radius, or angular momentum

(e.g., Symon, 1971). Hence, an object in a circular orbit of radius *r* from the Sun has the same total energy as an object in extremely eccentric orbits whose distance at aphelion can approach 2*r*. Due to this property, ejecta can be transported to beyond the orbit of Venus without adding any kinetic energy (Fig. 3).

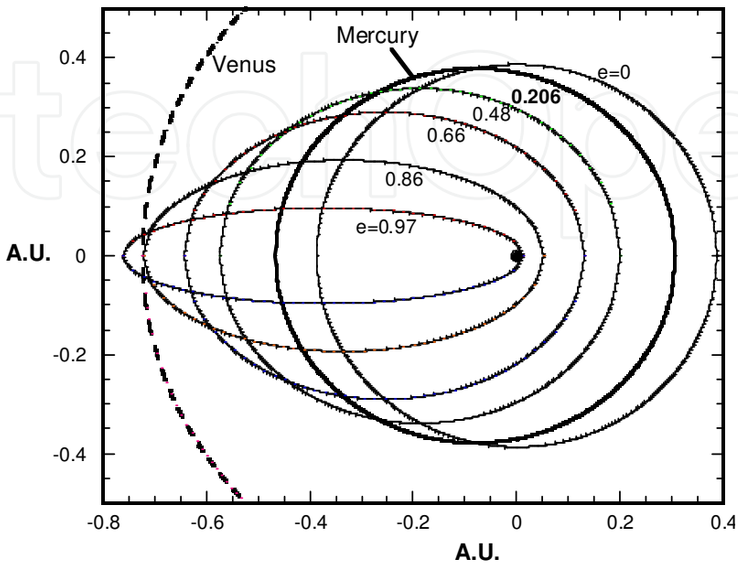

Fig. 3. Elliptical orbits for objects sharing the orbital energy of Mercury (solid curves, Mercury in bold), compared to the nearly circular orbit of Venus (dashed curve). Labels indicate the eccentricity of the orbits, which vary from a perfect circle (e = 0) to nearly unity.

3.2.1 Sling-shotting to distant reaches

For any ejecta, including those in elliptical orbits sharing the kinetic energy of Mercury's orbit, promotion to even more distant parts of the Solar System is possible. We base this remark on use of Jupiter's gravitational well to "slingshot" the famous Voyager spacecraft into the outer Solar System. If Venus were in a suitable position relative to the trajectories of ejected material in a highly eccentric orbit (e>0.86, Fig. 3), it is possible for that material with minimum kinetic energy to be promoted far beyond Venus' orbit.

3.2.2 Effect of kinetic energy beyond the minimum

If the perturbing collision adds energy to the object being ejected, far greater distances than Venus' orbit can be realized. Escape from Mercury itself requires 4.3 km·s^{-1}, a mere 1% increase over existing orbital energy. For transport to infinity, the velocity needed for an object to escape the gravitational well of the Sun at Mercury's orbit is 68 km·s^{-1}. Because the orbital speed of Mercury is 48 km·s^{-1}, escape of ejecta from the Sun's pull to infinity requires only doubling their kinetic energy. It should be clear that energies arising from impacts were sufficient to move material from the inner to the outer Solar System.

The kinetic energy of Mercury in its orbit is ~10^6 J·g^{-1} whereas that of the asteroids is much smaller, ~10^5 J·g^{-1}, because orbital velocities become progressively slower with distance from the Sun. Hence, material ejected from an inner planet, if on an appropriate trajectory, has

more than enough kinetic energy for placement in the asteroid belt. Once material reaches the belt, interactions and collisions with inward bound material could reduce their kinetic energy to an amount appropriate to the orbital energy in this region.

3.2.3 Solar controls on the draw of Mercury and on impact and ejecta trajectory

Geometry, properties of central forces, and relative sizes of Mercury and the Sun suggest possible paths. Importantly, gravitational competition with the Sun severely limits Mercury's draw. Due to the central nature of this force, for a particle within a dust cloud to be incorporated in a body orbiting a larger central mass (Fig. 4a),

$$\left(r_{\text{cloud}} / r_{\text{orbit}} \right)^2 \leq M / M_{\text{central}} \tag{3}$$

(Hofmeister and Criss, 2012). Although Mercury would actually draw in more distant material above and below its orbital plane and away from the Sun, our spherical formula suffices due to the large orbital radii and small planet mass: using the masses of the Sun and Mercury, provides a cloud size of 4.4×10^7 m, which is only 20 times Mercury's planetary radius (2.4×10^6 m) and an insignificant portion of its orbital radius (5.79×10^{10} m). Hence, a tiny spherical cloud reasonably describes the gravitational draw of Mercury. Impacts derived from cloud material are radial inward and help assemble the planet's mass. Our interest is rather collisions occurring after formation that would scour evolving Mercury.

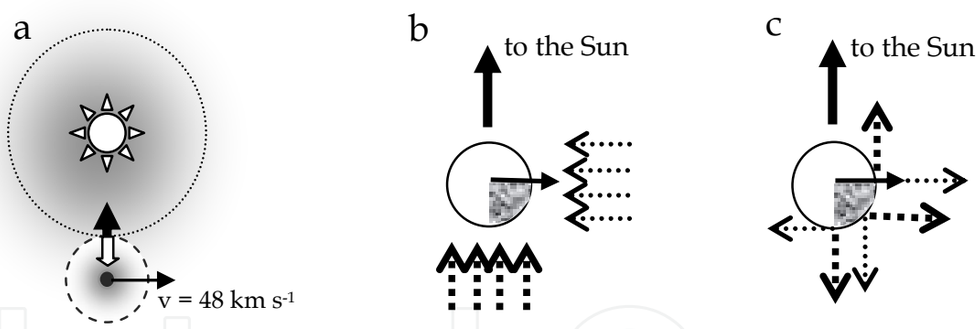

Fig. 4. Geometrical control on impacts on a planet. (a) Gravitational competition. The size of a cloud collecting unto an orbiting body (dashed circle) is determined by where the gravitational force (black arrow) of the central object (Sun) balances that (white arrow) of the orbiting protoplanet (dot). (b) Input trajectories. The planet (circle) in its orbit, intercepts material that is stationary or moving towards the planet (dotted arrows). Material focused on the Sun strikes the planet at nearly right angles (heavy dashed arrows). Shaded area = the most affected quadrant. (c) Initial output trajectories are shown for direct hits, glancing blows and strikes in the middle of the preferred quadrant.

Once Mercury was formed, two paths for impact are relevant. One is a "windshield" effect, whereby Mercury collides with debris entering its orbit (Fig. 4b). Because of the great distance to the Sun, these trajectories are approximately tangential to the orbit. The other impact path is approximately radially inward to the Sun (Fig. 4b), which is the gravitational focus of the Solar

System. Given the great distances, parallel paths reasonably approximate these impacts. Consequently, Mercury's outer leading quadrant is struck preferentially, and most of the resulting recoil paths point away from the Sun or are tangential to Mercury's orbit (Fig. 4c).

A minimum energy escape trajectory from an isolated body follows a parabolic path (e = 1). With increasing energy, hyperbolae are expected (e = 2; e.g., Symon, 1971). However, Mercury is not isolated and the Sun pulls ejecta with v < 68 km·s^{-1} into bound orbits (Fig. 5a). With more energy, the ellipse is larger, making excursion to the location of the asteroid belt possible for certain values of kinetic energy and initial paths. Aperiodic bounded orbits which exist for central forces (Symon, 1971) would be possible trajectory paths for intermediate energy particles, with initially tangential trajectories (Fig. 5b). This type of orbit can be open as shown, or closed, similar to the patterns of a drawing implement known as a "spirograph." Orbits of meteor strikes are presumed ellipses (e.g., Gounelle et al., 2006). To our knowledge, aperiodic bound orbits have not been considered, yet these are not only less restricted by geometry but are more likely to intersect Earth over time.

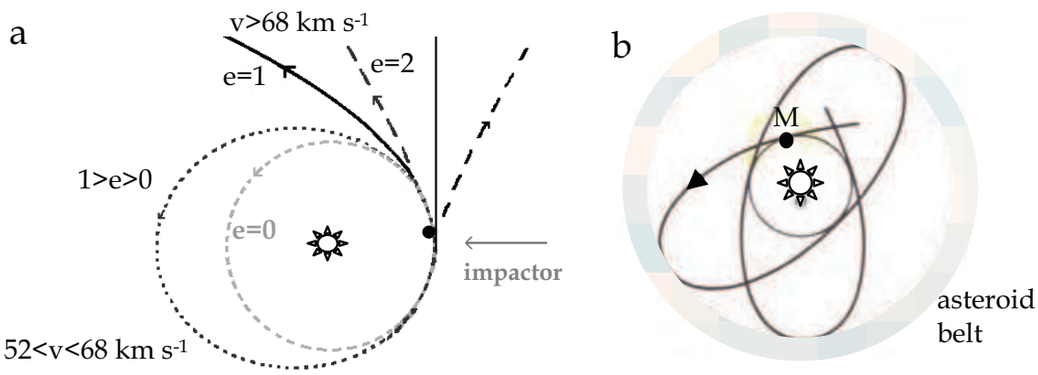

Fig. 5. Schematic of possible ejecta orbits. (a) Simple orbits showing the connection of eccentricity with velocities needed to escape the Sun's control. Only for v>68 km·s^{-1} can the ejecta escape the Solar system. (b) Aperiodic bound orbits are permissible for a central force (Symon, 1971) and could arise from initially tangential recoil paths.

3.3 Mass arguments for the asteroid belt as debris

Regular and distinct trends exist for the mass of dusty and gassy bodies that orbit the Sun with distance (Fig. 6). These trends result from 3-d accretion of the pre-solar nebula (Hofmeister & Criss, 2012), such that the dusty bodies form first, and gas is augmented onto dusty protoplanets in accord with Eq. 3. The decrease in mass for the dusty bodies going as $r^{-1.7}$ is consistent with conservation of angular momentum and energy during 3-collapse. Independent of our model, the trend for dusty primary satellites shows that objects in the asteroid belt formed in a different manner than did the planets and dwarf planets, especially insofar as the total mass in the asteroid belt falls two orders of magnitude below the trend.

3.4 Type and mass of material excavated from evolving Mercury

The innermost planet seems to have lost practically all of its mantle, as its core extends out to nearly 80% of the planet's radius, and constitutes ~⅔ of its total mass (Fig. 1). A plausible interpretation is that proto-Mercury was once at least as large as Mars (Fig. 1) and that

>3x10^{23} kg mostly of silicates was blasted off this battered planet early in its history. The total mass of the asteroid belt (~3x10^{21} kg) is only 1% of Mercury's loss, and half of the mass in the belt is sequestered in one object, Ceres. Much of Mercury's lost mantle would have been absorbed within the inner Solar System, but this huge quantity of material will offset the low probabilities of ejecting material and transferring it to Earth-crossing orbits. Transport of <1% of Mercury's loss to the asteroid belt is reasonable, and, more importantly, is much more than sufficient to generate the aggregate mass of achondrite and other classes of meteorites in available collections, including the ~1000 kg of HEDs (Table 1). Other bodies will provide achondritic material, but in much smaller amounts and ejecta originate at various times. Chondritic material would represent dust originating from this region.

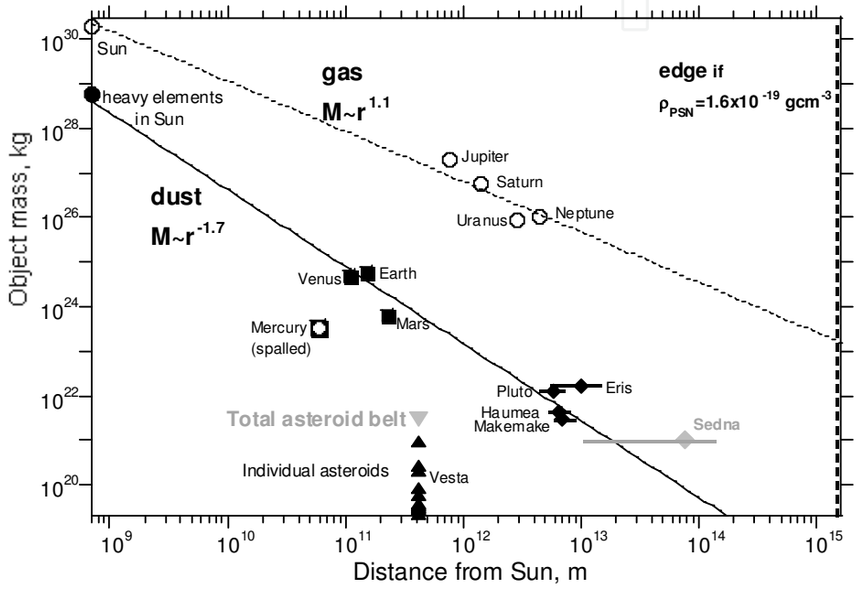

Fig. 6. Mass of large bodies orbiting the Sun vs. distance from the origin. The Sun is plotted at its body radius to use a logarithm plot, needed to represent the vastness of the Solar System. Open circles and dotted line = gas giants. Dashed line at right side = radius of the pre-solar nebula, calculated from the Sun's mass, assuming an initial density like that of molecular clouds. Filled circle = heavy elements in the Sun (Basu & Antia, 2008), taken to represent the dust component of the pre-solar nebula (PSN). Squares = inner rocky planets, except Mercury (open square) which has lost significant mass. Diamonds = dwarf planets of the outer Solar System. Line = fit to the circles, squares and diamonds. Grey diamond = Sedna. Horizontal lines describe substantially elliptical orbits. Triangles = individual asteroids (grey for the total mass). Data from Lodders & Fegely (1998) and http://pds.jpl.nasa.gov/.

The heavily cratered surface of Mercury and its location as the innermost planet provide evidence for deep excavation. Saturation of the surfaces of Callisto and Ganymede with craters implies that the Jovian moons were also extensively bombarded, due to the gravitational focus of impactors by Jupiter. By analogy, early, evolving Mercury received an intense flux of impactors, due to its proximity to the Sun.

Our understanding of impacts is skewed toward late, low energy events which do not cause great loss of planetary matter. Such minor impacts provide dust (rayed craters), breccias,

shock metamorphism, large volumes of melt, and small volumes of melt ejecta (tektites and small spherules) (French, 1998). Mercury has low gravity and lacks an impeding atmosphere. Impacts into pools of melt on Mercury splattered innumerable chondrules into space. Crystallization of the melt in space would provide round rather than the aerodynamic shapes of tektites, and would have formed bodies of diverse sizes. More massive impacts would have vaporized material, which would have escaped and then condensed. The internal structure of Mercury suggests that most ejecta would be from the mantle. However, impacts add their own matter to the surface, which would also be subsequently ejected. Hence, primitive material, differentiated material, both their melts, and mixtures of all such debris are possible. Vesta could be a conglomerate of ejecta from Mercury.

3.5 Statistical arguments for planetary origins of meteorites

Asteroids are classified by remotely sensed data by several schemes. Spectra (Bus & Binzel, 2002) or spectra plus albedo (Tholen, 1989) are further used to link these types to meteorites. Broad categories of asteroids common among these schemes occur in percentages that are inconsistent with the numerical occurrence of meteorites (Fig. 7). Current collections have ~40,000 samples (Table 1) and should be statistically representative. Mass distribution gives us a different perspective and is skewed towards high iron content, due to material strength. Also, spectra of asteroids preferentially represent larger bodies.

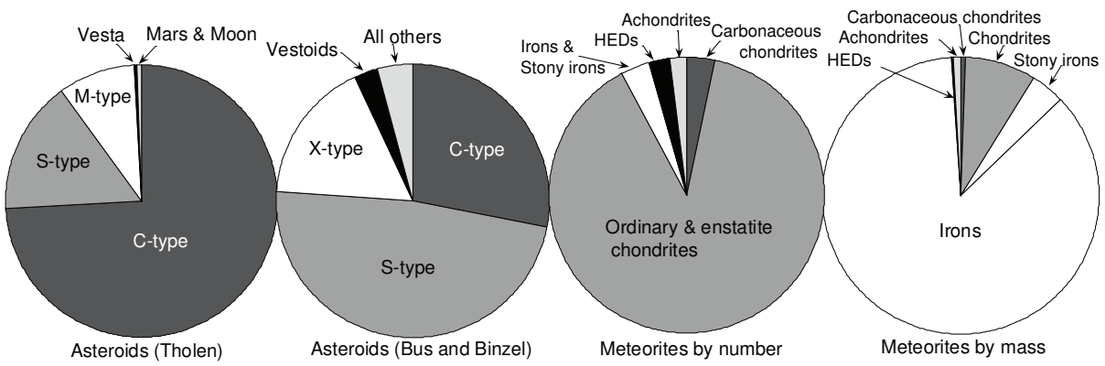

Fig. 7. Large disparity between two different asteroidal classifications (left) and meteorite types (right). Dark "C-type" asteroids represent a majority, yet are considered as the primary sources of the rare carbonaceous chondrites. Vesta is only one of $>10^6$ asteroids, but is presumed to be the source of the HEDs, which represent >½ of the achondrites, and are geochemically tied to ~ ⅓ of the irons, and most stony-iron meteorites. Data from Table 1.

The current linkage is statistically untenable, as is well known. Problems exist with attribution of C-type asteroids to carbonaceous chondrites. Spectra of C-types are featureless with low albedo, consistent with dusty surfaces; it may simply be that their mineralogy is equivocal. Grain-size and dust coverage affect surface spectra (Section 4).

3.6 The asteroid belt as the junkyard of the Solar System

The above dynamical, mass, and statistical considerations lead to an alternative view of the asteroid belt. Classical mechanics requires that ejecta from early Mercury predominately

occupy elliptical orbits and aperiodic bound orbits. Over time, the amount of material is non-circular orbits will diminish. The inner Solar System has been swept clean. The asteroid belt has a large number of objects because the distances are large, so the clearing rate is low, and a planet did not form in this area. On this basis, a likely repository for the ejecta and leftovers of accretion is the asteroid belt. Gravitational forces (e.g. Jupiter) have shepherded errant objects into this veritable junkyard of debris. Nothing requires this zone to be the locus of accretion for all of its material.

4. Limitations of spectroscopic assignments

Spectra from remote objects are obtained under uncontrolled conditions and contain a mixture of absorption, emission, and reflection features. To relate these data to laboratory mineral spectra, we need to understand how spectra are affected by sampling conditions.

4.1 Effect of temperature on spectra

For a remotely probed surface, the most important effect of temperature (T), is the control it exerts on whether the object is emitting or reflecting light over any given frequency range.

Blackbody emission curves depend strongly on T and frequency (Fig. 8a). The 1st law of thermodynamics requires that the flux from Vesta match that received from the Sun (Fig. 8b); roughly speaking, the areas under the curves must be equal. Due to the properties of Planck curves, Vesta, which is cold (85<T<255 K; e.g., Lucey et al., 1998) outputs virtually all its light below 2200 cm^{-1}, and therefore is emitting in the infrared but reflects light in the near-IR to visible.

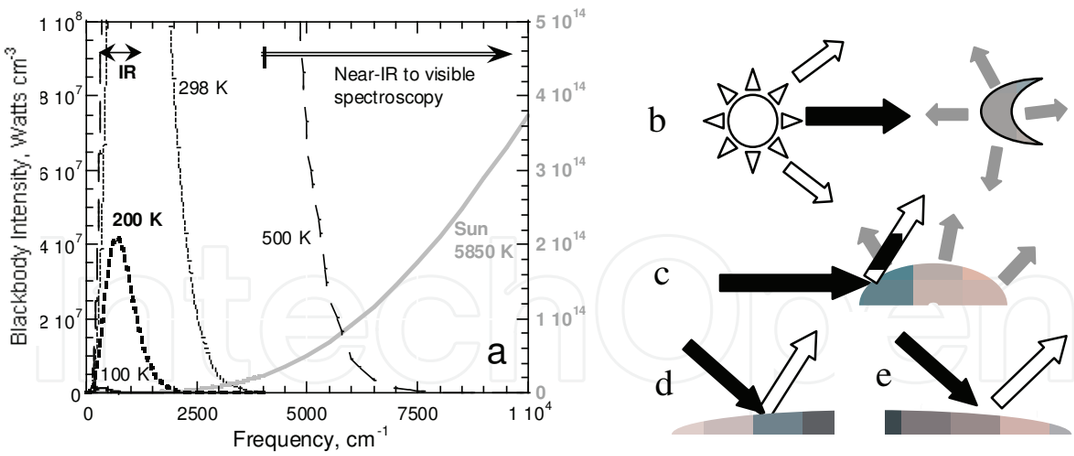

Fig. 8. Factors governing whether light is emitted or reflected. (a) Dependence of blackbody curves on temperature, as labeled. Except for the Sun at ~6000 K (grey), the left y-axis pertains. Arrows indicate spectral ranges sampled by different instruments. (b) Schematic of the first law of thermodynamics. Black arrow = light from Sun. Grey arrows = light emitted, which integrated over the area and frequency must equal the flux received.
(c) Cold objects emit at low frequency, and reflect sunlight at high frequency (speckled arrow). Both are modified by spectral properties, which depend largely on whether the surface is bare (d) or dusty (e), as sketched for the case of reflected sunlight.

4.2 Effect of grain-size on spectra

Grain-size controls whether peaks are superimposed positively or negatively on the baseline, and strengths of the features.

Light produced by a body at any frequency is the product of the blackbody function times the emissivity. Kirchhoff's law for a body in thermodynamic equilibrium requires that absorptivity ($\alpha = I_{abs}/I_0$, where I_{abs} = the intensity of light actually absorbed) equals emissivity (ε) (e.g., Bates, 1978; Brewster 1992). For an opaque material such as a metal, $1 = \alpha + r$, where $r = I_{ref}/I_0$ is reflectivity. Although asteroids are large and opaque, dust grains on their surface are partially transparent. For the part of the asteroid that is sampled, $1 = \alpha + r + t$, where $t = I_{tran}/I_0$ is transmittivity of the uppermost layer as derived by Bates (1978) for dielectrics (e.g. silicates).

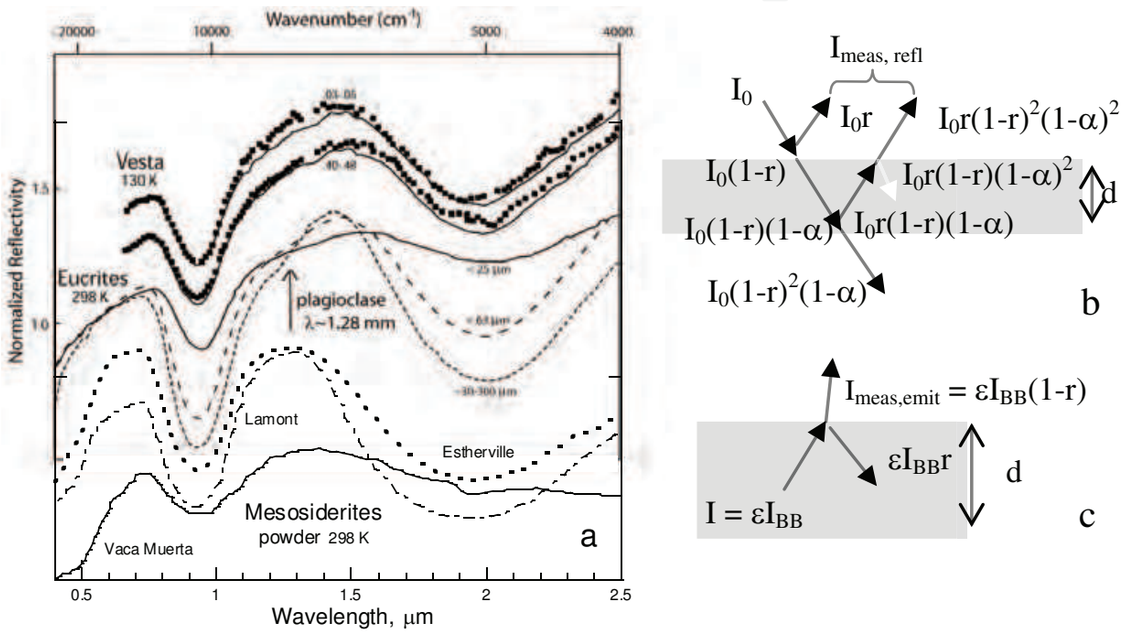

Fig. 9. Effect of grain-size. (a) Comparison of orientational differences in spectra for Vesta to the grain-size dependence of reflectance-absorbance spectra from eucrites [solid = Padvarminkai (Hiroi et al., 1995); dashed = Macibini (Burbine et al. 2001); dotted = Padvarminkai (Gaffey, 1976)] and powdered mesosiderites as labeled (Burbine et al., 2007). Vesta spectra (Gaffey, 1997) are shown for two rotational aspects (dots), with each compared to the average (lines) of 4 to 5 rotational aspects. The uncertainties are roughly 2-3 times the symbol size, and the placement of the points near 2 μm is not exact because spectra presented at different scales were merged. Spectra offset for clarity. (b) Schematic of reflections for the most intense ray paths at near-normal incidence (the angle is exaggerated and the white arrow is not labeled). The light received by a detector (I_{meas}) relative to incident intensity (I_0) is a combination of reflection and absorption, depending on thickness, d. (c) Schematic of emissions, where I_{BB} is blackbody intensity.

Measurements are affected by back reflections (e.g., Hofmeister et al., 2003). If the surface layer is very thick then the back reflections are not sensed. Reflectivity at high frequency is flat for a bare, large, single crystal due to Fresnel's law, ($r = [(n-1)^2+k^2]/[(n+1)^2+k^2]$ where n is the index of refraction, $k = a/4\pi\nu$ where a is the absorption coefficient, and ν = frequency.

For grain sizes of rocks, measured reflectance is reduced by back reflections (Fig. 9b). As spectra of eucrites demonstrate (Fig. 9a), larger grain size at the surface means deeper absorption features. Small grains are not detected: these contribute only to scattering.

Regarding emitted light, for a bare, thick surface or large grains, $\varepsilon = \alpha$, so emissions go as $I_{BB}(1\text{-}r)$. At frequencies where transitions occur less light is received, i.e., peaks point down as seen in the spectra of Christensen et al. (2000). (Note: 1-r has been incorrectly interpreted as emissivity for large grains). If the surface is covered with dust, this layer is heated by lattice conduction from below and emitted light comes only from this layer. Because reflection peaks are broader than absorption peaks, emissions from a dusty surface go as $\varepsilon I_{BB} = \alpha I_{BB}$ and peaks point up as seen in spectra from small grains (Low & Coleman, 1966; Bates, 1978) and references therein.

4.3 Effect of Fe^{2+} contents and grain-size on near-IR reflectance spectra of Vesta

High frequency reflection spectra (Fig. 9a) have the strong peaks of pigeonite (as in eucrites). Fe-bearing plagioclase may be present: its 8000 cm^{-1} band (Hofmeister & Rossman, 1984) is weak for Serra de Magé eucrite. No obvious peaks for orthopyroxene (dioginites) or olivine (pallasites) exists. Such may be extracted by peak fitting, but variations in grain-size of pigeonite suffice to explain the scant differences, as is clear from Fig. 9. Variation in grain-size were inferred from recent analysis of Vesta's mid-IR light-curves (Chamberlain et al., 2011).

Mesosiderite spectra are similar to eucrites, but the presence of orthopyroxene broadens the peak at 2000 nm and shifts it to 1800 nm (Fig. 9). The surface of Vesta was impacted. Rapid surface cooling would produce pigeonite as in terrestrial lavas. From Fig. 9, the surface of Vesta could be a mixture of pigeonite and metal. The proportion of pigeonite is high, based on peak depths, which is consistent with Vesta's density (Section 1.1.1).

Importantly, the depths of the peaks are connected with Fe^{2+} content of the minerals. Orthopyroxene in the HEDs has Fe/(Mg+Fe) of 0.25 which is half that of pigeonites. Therefore, pigeonite will dominate if in equal proportions. Orthopyroxene is also coarse grained: large crystals will not provide back reflections. The spectra of Vesta could contain all phases of mesosiderites, but spectra only prove that pigeonite is present and abundant.

4.4 Problems with interpretation of mid-IR emission spectra from Vesta

Spectra obtained of Vesta using the Infrared Satellite Observatory (ISO) record its emitted light. A broad peak near 450 cm^{-1} (Heras et al., 2000) indicates a blackbody temperature of 130 K, consistent with previous inferences (e.g., Lucey et al., 1998). ISO spectra in this range and below are noisy, obscuring features of minerals. Mid-IR features are weak, consistent with a dust covering (Dotto et al., 2000; Lim et al., 2005). Hence, these features are in emission. Unfortunately, spectral analyses by these authors assume that emissions are that of an opaque (metallic) body [= $I_{BB}(1\text{-}r)$] whereas presence of a dust cover requires that $I_{meas,emit} = \varepsilon I_{BB}$ for a dielectric (silicate) material (Fig. 9bc). The fits need redoing.

5. Geochemical arguments for HEDs as inner Solar System material

Meteorites display a bewildering complexity of chemical and isotopic relationships. The following discussion focuses on characteristics that reveal radial chemical gradients in the

Solar system inherited from the pre-solar nebula. An important marker is the ratio of volatile to refractory elements, which is exemplified by K/U and Rb/Ba ratios. A ratio involving Al is useful because this refractory element has a short-lived isotope. We selected Ga for normalization as it is a more volatile Group IIIA element with a similar ionic radius.

Stable isotope ratios (e.g. Si, O) have proven utility to petrogenesis. Oxygen isotopes are exceedingly important because this element is abundant and its fractionation and distribution are well-understood.

5.1 Geochemical characteristics of meteorites

Detailed descriptions of the geochemical and petrological characteristics of HED meteorites are available (see references in Section 1.1). Compared to other achondritic meteorites, the HED family includes the oldest known basalts in the Solar System, is the most volatile depleted, the most strongly reduced, and distinct in terms of isotopes (Table 2).

Ordinary chondrites, by far the most abundant stony meteorites (>90%), are widely believed to originate from the asteroid belt. This attribution is consistent with chemical uniformity of this group of meteorites. Persuasive arguments for the origination of SNC meteorites from Mars have been advanced (see Grady, 2006). In contrast, assigning the HED family to Vesta or Vestoids (e.g., Drake, 2001) contradicts physical data (Section 1), abundances (Fig. 7), and geochemical characteristics, discussed below.

	A.U.	K/U	Rb/Ba	10^4 Ga/Al	$\Delta^{17}O$	$\delta^{18}O$	$\delta^{30}Si$
R chondrite	~3	>40000	>0.35	8	2.8	4.3	
Ordinary chondrites	2-3	60000	0.6	5	0.7 to 1.3	3.7 to 5.6	-0.46
Mars, SNCs	1.52	16000	0.17	4	0.27	4.5	-0.48
Earth upper mantle	1.00	10000	0.10	2	0.00	5.7	-0.68
Moon, Lunar	1.00	3000	0.015	0.3	0.00	5.7	-0.45
Venus	0.72	7000*					
HEDs, protoMercury	0.39	3700	0.007	0.2	-0.25	3.7	-0.45
Ureilites, CAI, K-ch	~0	<1000	0.002	0.005	<-0.8	<8.1	-0.47

Table 2. Geochemical and isotopic characteristics of meteorites and rocky planets. Data Sources: BVSP (1981), Lodders and Fegley (1998), Lodders (1998), Kitts and Lodders (1998), Molini-Velsko et al. (1986), McKeegan et al., (1998); MacPherson et al. (2005), Franchi et al. (2008), Armytage et al. (2011) and others. For A.U.~0, oxygen values were taken from a cluster of ureilites and a chondrule from the Kakangari chondrite (Prinz et al., 1989). For R chondrites, the average excludes hot desert finds. *Gamma ray spectrometer results for Vega 1 and 2 (Surkov et al., 1987).

5.2 Chemical trends in the Solar System

The trends in Table 2 are coherent and regular. Similarities in the K/U ratio among disparate rock types on Earth, and the large difference of this ratio from that in chondrites, were established long ago by Wasserburg et al. (1964).

Note that the K/U ratio of HED meteorites is much more similar to rocky materials from the inner Solar System than it is to materials presumed to have originated outside Earth's orbit.

The Rb/Ba ratio is also consistent and characteristic for each of the rock suites under consideration (Fig. 10). This and the Ga/Al ratio increase markedly in the order that the K/U ratio increases (Table 2). The remarkable coherency of Rb/Ba ratios in lunar materials, which are distinct from the chondritic ratio, has been demonstrated (BVSP, 1981, p. 251).

5.2.1 Attribution of the HEDs to protoMercury: implications for elemental compositions

Not all element ratios will vary in the same manner as those in Table 2, nor would such coherency be expected given the profound differences in planetary masses, timescales and extents of differentiation, and other factors. What is remarkable, however, is that so many compelling geochemical signatures vary in the same order, with the HED family near one extreme. These regular variations involving both major and minor elements, as well as the stable isotopic variations of the most abundant elements, are consistent with an origin from the inner Solar System, most logically, from early Mercury. The inventory of volatile and large ion lithophile elements in protoMercury would have been greatly reduced by spalling, leaving a remnant planet highly depleted in these elements, including K, U, and Th. Chemical data provided by Nittler et al (2011) and Peplowski et al. (2011) confirm our deduction.

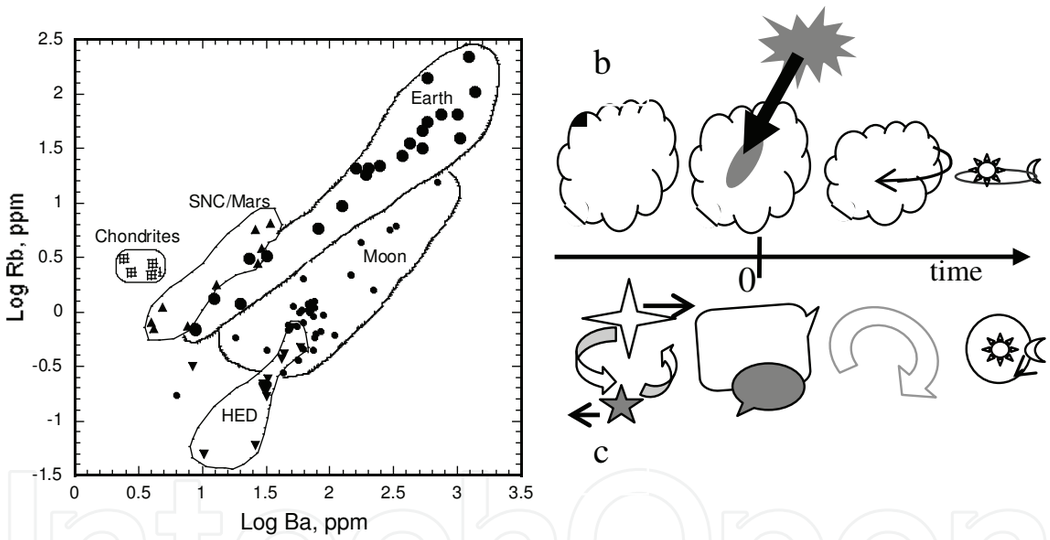

Fig. 10. Zonation in the pre-solar nebula. (a) Rb vs. Ba concentrations for Solar System materials, suggesting HEDs are refractory inner Solar System material. Sources as in Table 2. (b) One hypothesis for origination of the zonation. From left to right: the pre-solar nebula of dust and gas (white cloud) is stable, but a nova injects material (grey) including refractory CAIs, while producing or inducing short-lived isotopes such as ^{26}Al (grey). The injection diffuses, but the center of its mass provides a gravitational instability, precipitating nebula contraction, rotation around this locus, and planetary accretion. (c) Alternatively, two passing and interacting stars provide distinct reservoirs of dusty gas.

5.3 Oxygen isotope variations in the Solar System

Graphs of $\delta^{17}O$ vs. $\delta^{18}O$ values of achondrites and other meteorite types (Fig. 11) display a lattice-work of 1:1 and 1:2 lines, which respectively represent a mass-independent

fractionation trend and an ordinary mass-dependent fractionation trend. Practically all Solar system materials lie between the 1:1 lines known as EC (Equilibrated chondrites) and CCAM (carbonaceous chondrite anhydrous minerals). The CCAM line includes CAI inclusions from Allende which are very old, refractory, were rich in short lived isotopes and extend to incredibly low values. CAIs from enstatite and ordinary chondrites have similarly low values (McKeagen et al., 1998; Guan et al., 2000). Several lines of evidence point to CAI's being near the center of the Solar System and representing a distant reservoir (MacPherson et al., 2005).

The 1:2 trends are superimposed on the 1:1 trends and are due to ordinary fractionation processes that continue today on Earth (the TFL). For any given planet, surface materials will lie to the upper right along these 1:2 lines (Fig. 11), while deep interior materials will lie to the lower left. Mars' meteorites lie above the TFL, whereas the HEDs lie below by a similar amount. These 1:2 trends develop during late stage heating of formed bodies by various processes and may onset early from impact heating

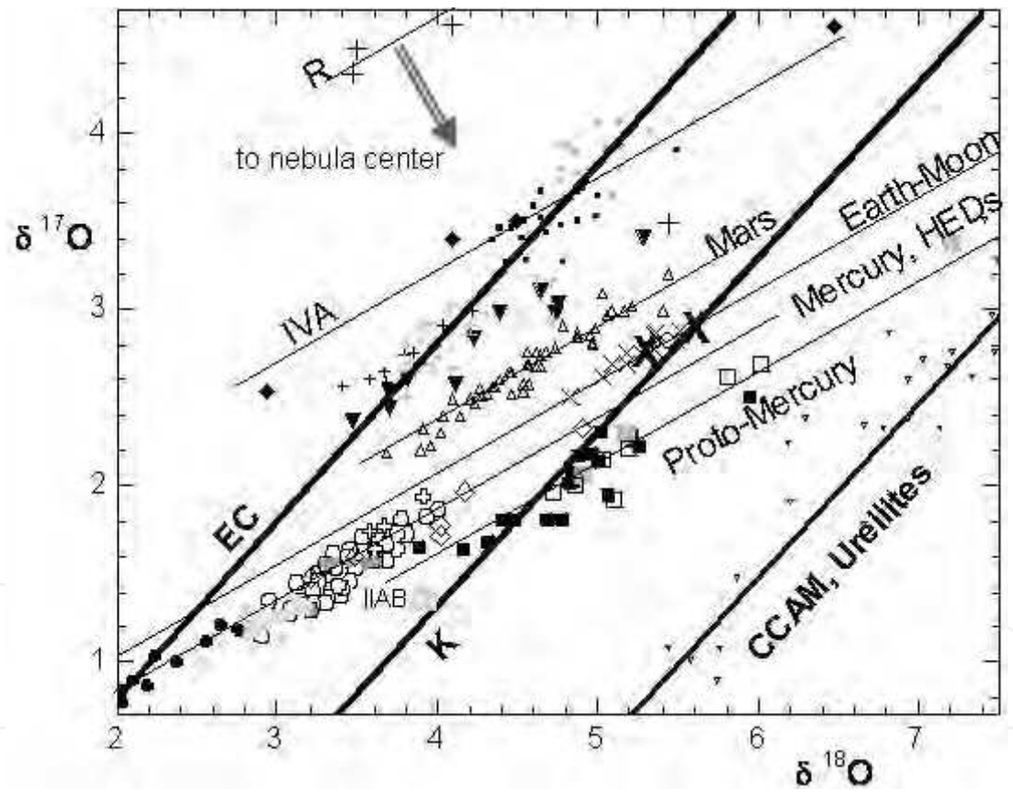

Fig. 11. Oxygen isotopes. Tiny triangles = ureilites. Open squares = winonaites. Grey square = IIICD irons. Black squares = IAB irons. Circles = HEDS. Dark grey dots = mesosiderites. Light grey dots = main group pallasites. Black dots = IIIAB irons. Open cross = angrites. Open diamond = brachinites. Light X = aubrites. Heavy X = enstatite chondrites. Open triangles = Mars meteorites. Filled triangles =IIE irons. Filled diamonds = IVA irons. Small plus = H chondrites. Tiny black squares = L chondrites. Tiny grey squares = LL chondrites. Large plus = R-chondrites. Light lines = fractionation trends for various bodies, as labeled. Heavy lines = solid-gas interaction, as labeled. Double arrow indicates the Solar System gradient. Data from Clayton and Mayeda (1996); Franchi et al. (2008); and other sources.

6. Geophysical implications

To obtain bulk compositions of the silicate Earth and its core requires coherently explaining Fig. 11 in general terms that are consistent with fundamental principles and the data, and understanding the assembly, spalling, and resultant layers of Mercury.

6.1 Attribution of the HEDs to evolving Mercury: implications for layer compositions

The large size of Mercury's core shows that it was deeply spalled both during and after core formation. Spalling was caused by late-stage impacts from the outer Solar System (Section 1.2), which added material from distance because impactors bury themselves while ejecting target material (French, 1988). Thus, the HED family trend lies closer to the TF line than proto-Mercury did. The upper layers of early Mercury must be represented in the meteorite collection. The trend of winonaites, IAB and IIICD irons lies below the HEDs (Fig. 11). This material is more pristine, consisting of non-magmatic irons and is similar to the enstatite chondrites associated with the Earth (e.g., Javoy, 1995) corroborating proto-Mercury as the source.

The HEDs represent early Mercury's present mantle, the mesosiderites are a combination of poorly sorted core-mantle boundary material and late-stage additions, and the IIIAB irons represent core material. Main-group pallasites represent material ejected from the zone of gravitational settling during core formation. Approximate compositions are in Table 3.

Object or layer	**Meteorite analogy or composition**
Proto-Mercury	Winonaites + IAB + IIICD + ices
Bulk silicate early Mercury	HEDs
Core-mantle sorting	Pallasites, main group
Mercury's evolving core	IIIAB
Proto-Earth	enstatite chondrites + ices
Bulk silicate Earth	½ enstatite chondrites + ½ ordinary chondrites + ices
Earth's core	~85%Fe + ~5%Ni + ~10%C with minor S, N, P

Table 3. Zones in Mercury and Earth and their connections with meteorite types.

6.2 Explanation of solar system gradients and trends

We dismiss the hypothesis that the material which formed the planets post-dates the Sun. The "condensation gradient" is invalid in view of recent data on comets (Zolensky et al., 2006). Simultaneous formation of the Sun and planets by 3-d nebular collapse is supported by the axial spins and orbital characteristics of the planets (Hofmeister & Criss, 2012) and indicates rapid accretion over ~1-3 Ma. What did the Solar System form from? Pre-solar grains indicate diverse sources (Bernatowicz & Zinner, 1997). For simplicity, given Table 2 and Fig. 11, we consider that two reservoirs of dust existed, which were embedded in an immense reservoir of gas. Gas constituents are mostly H_2 with He and CO. Its mass is ~100 times larger than the dust mass, based on solar composition (Basu & Antia, 2008).

Our analysis is also based on the mineralogy of dust in astronomical environments. Infrared dust emissions of the exploded circumstellar dust of NGC 6302 contain many peaks,

consistent with the presence of pure, magnesium endmember silicates (forsterite, enstatite, and diopside), possibly calcium carbonate (Molster et al., 2001; Kemper et al., 2002), along with CAI minerals (Hofmeister et al., 2004). Hydrosilicates are possible (Hofmeister & Bowey, 2006). Dense dust clouds around young stellar objects contain ices (H_2O, CO, CO_2, CH_4, hydrocarbons) thought to nucleate on the dust, summarized by Bowey and Hofmeister (2005) who identified melilite (a CAI phase) and Mg-rich amphiboles (hydrated pyroxenes).

Both dust reservoirs condensed from hot gas expelled from pre-existing stars (Fig. 10bc). The large, and possibly pre-existing, dust reservoir involves O, Mg, Si, Fe, consistent with major elements in the Earth and with stellar nucleosynthesis. This reservoir is exemplified by the ordinary and R chondrites and dominates the outer reaches (Fig. 12). The large dust reservoir also contained lesser amounts of high-temperature phases, and lower temperature phases with volatile elements. The small, probably injected, dust reservoir provided the CAI inclusions, short-lived isotopes, refractory elements, and lesser amounts of iron and other materials which dominate the large dust reservoir. For a simple explanation of the 1:1 trends, we assume that the gas phase is greatly enriched in ^{16}O.

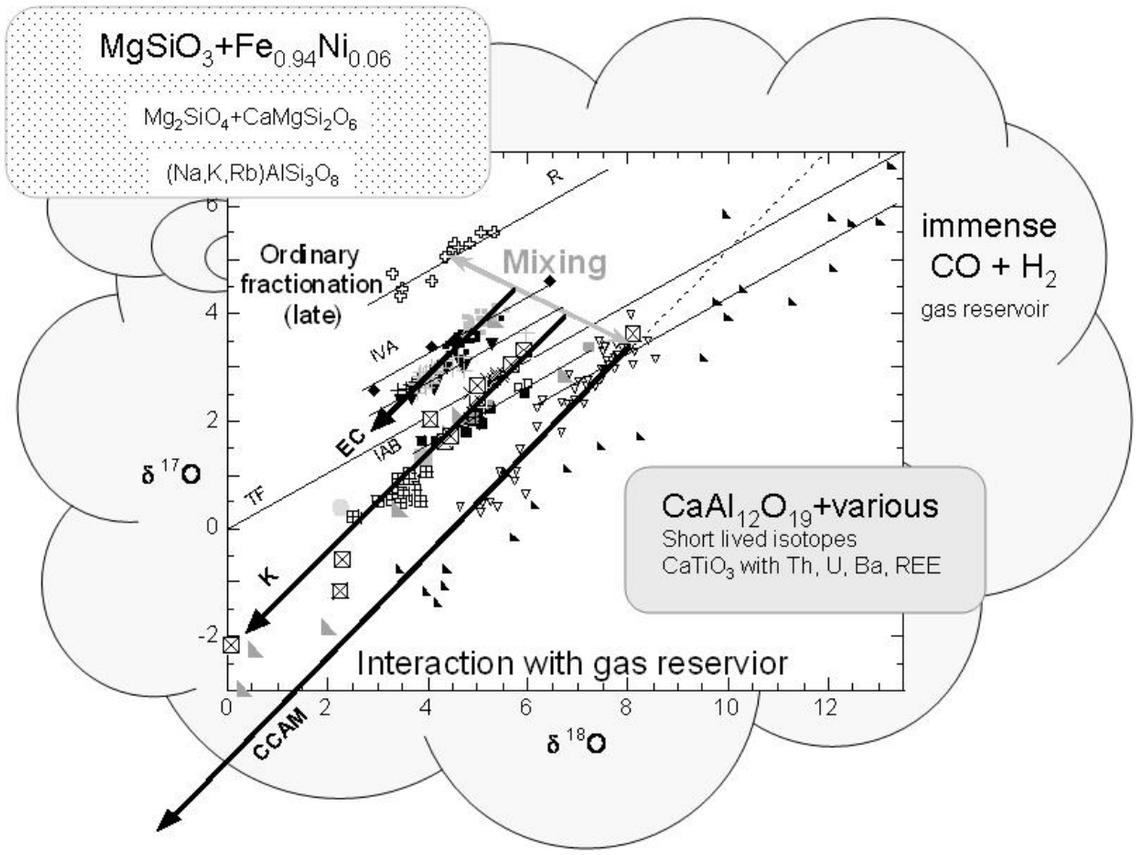

Fig. 12. Reservoirs and processes altering oxygen isotopes and mineral phases and compositions. Symbols for meteorites as in Fig. 11 with the exception of open cross = R-chondrites, and a few additions: Square with cross = acapulcoites. Square with X = K-chondrites. Right triangles = dark inclusions in CAIs. Light lines = late, ordinary fractionation within the various bodies, as labeled. Heavy lines = mixing or gas fractionation, as labeled. Grey double arrow indicates the Solar System gradient.

Upon assembly of the planets, and heating via impacts or radioactivity, dust in the main reservoir reacted with trapped ices, exemplified by CO:

$$2Fe^0 + CO + MgSiO_3 \text{ (enstatite)} \rightarrow FeC + (Mg,Fe)SiO_4 \text{ (olivine)}. \quad (4)$$

This reaction converted end-member pyroxene to solid-solution olivine. The isotopic drive was towards the CO reservoir, which was rich in ^{16}O. This reaction is germane to core formation, suggesting that carbon is the core's light element, consistent with solar abundances. Earth's core has ~10% light elements, mostly C, consistent with ubiquitous occurrence of olivine with Fe/(Mg+Fe) ~ 0.1 in meteorites, mantle samples, and terrestrial basalts. Equation 4 and similar reactions provide for enrichment of Ni accompanying incorporation of C, S, N and P in the core while lithophiles (e.g., Ge and Ga) are transferred to the silicates. Comparison of the composition of IAB to IIIAB irons associated with evolving Mercury (see Mittlefehldt et al., 1998) supports our proposal.

The small dust reservoir (CAIs, ureilites) has many phases and many reactions are possible. Because metals that condense at high *T* are rare (e.g., V, Mo, Nb, Pt group), reactions similar to Eq. 4 in the small reservoir could go to completion. Melilite could be converted to forsterite and fassitic pyroxene would be formed, for example. Without ample Fe^0, the following reaction is suggested to be important with dust serving as nuclei:

$$CO + H_2 \rightarrow C + H_2O. \quad (5)$$

Metals such as V were incorporated in hibonite, ample graphite was produced, material was hydrated and/or carbonated, and the CAI phases were mass-independently fractionated.

Reactions like Eq. 4 and 5 proceed with time and this sequence is recorded in meteorities which were ejected from evolving Mercury and other planets as the late stages of accretion progressed. Nearly full-formed planets provided the ejecta, in accord with early assembly involving dust, with large impacts being associated with the late influx from great distance (Hofmeister & Criss, 2012). The earliest ages deduced from isotopic studies correspond to condensation of the dust reservoirs from their stellar sources. Early chondrule ages (Amelin et al., 2002) of 2.5 Ma later record the onset of large impacts, and the end of proto-planet assembly, consistent with Hofmeister and Criss' (2012) analysis using the time-dependent virial theorem.

Mixing of these two dust reservoirs created a graded solar system (Figs. 11 and 12). Because of contraction and events like the LHB, the proportion of the main (outer) reservoir increased with time. The EC line pertains to the asteroid belt, whereas the K line pertains to the dust in the inner Solar System. The current planets lie about half way between these 1:1 lines. To this, CO and H_2O and other ices, which were frozen on dust drawn into protoplanets, were added in indeterminate amounts.

6.3 Fractionation trends and evolutionary processes

After assembly of the bodies and heating, mass-dependent fractionation occurs, superimposing lines parallel to TF for individual planets and large masses. All 1:2 lines for meteorite types are about the same length, consistent with similar thermal histories of the body after ejection to the asteroid belt. The longer line for the HEDs and related meteorites is consistent with origination in Mercury, given that the large Earth has an even longer 1:2 line. The degree of ordinary fractionation directly depends on the mass of the object (Fig. 13).

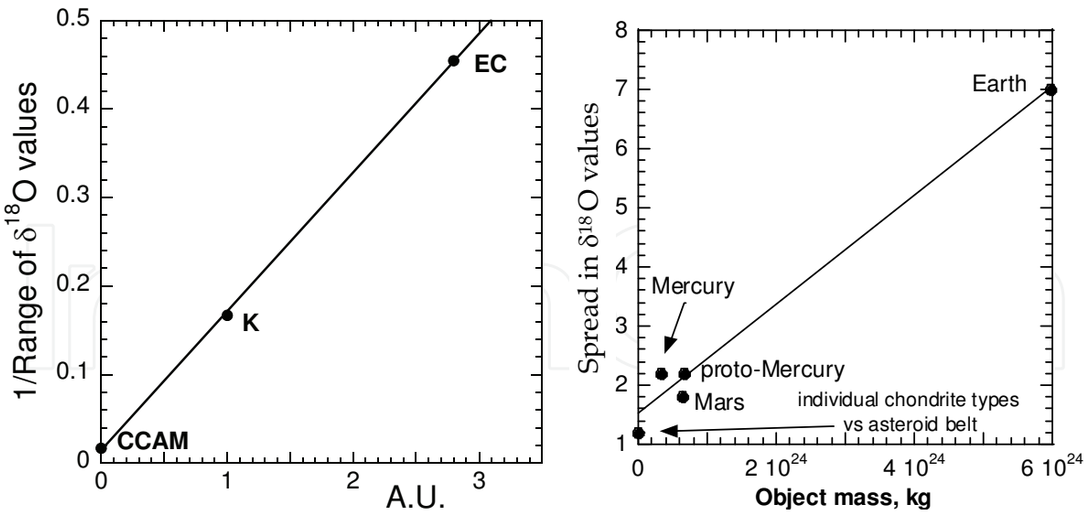

Fig. 13. Dependence of mass dependent fractionation on mass and of the inverse mass-independent fractionation on distance from the center. Objects and fractionation trends as labeled.

This trend is consistent with larger bodies being hotter and staying active longer. This trend may aid in deciphering parent bodies.

In contrast, the inverse of the length of the 1:1 lines depends on distance from the nebula center (Fig. 13). This important new finding corroborates that the small reservoir with short-lived isotopes was indeed at the center of the nebula, and suggests that our Solar System formed after a nova. Involvement of a second star is mandated by the existence of two dust reservoirs. The 1:1 line lengths could be derived from light-energy from the nova.

7. Conclusions and future research

We provide an alternative view of the origins of meteorites and the asteroid belt, based on fundamental principles. The connection of HEDs and related meteorites with early Mercury provides a coherent view of the ~40,000 samples of meteorites, suggests new relationships with the planets, and provides a consistent picture of their formation. Our analysis removes guesswork in estimating chemical compositions for the planets and provides many testable predictions to guide future work:

- The light elements in the core are C, S, N and P.
- Core formation involved redox reactions dominated by C, and released divalent iron into mantle minerals. This process increased the proportion of olivine to pyroxene.
- The $\delta^{18}O$ values of Earth are vertically zoned, with the lower mantle being lower in ^{18}O than the upper mantle. Earth's bulk $\delta^{18}O$ value is close to +4.
- Carbonaceous chondrites are too refractory to describe the Earth's composition.
- The smaller the object's core, the more Fe-rich the basalts.
- The oxygen isotope composition of Mercury will be shown to be similar to that of the HEDs.
- Asteroid 4Vesta is a mesosiderite that has undergone minor surface melting and rapid quenching due to impacts.

- Studies of Vesta's moment of inertia will disclose that it is internally homogeneous and lacks a core.
- Many Earth-crossing orbits are not elliptical but aperiodic bounded orbits.
- Properly analyzed emission spectra will help correct the asteroid classification system.
- All differentiated meteorites will be eventually linked to planetary bodies and other large objects such as the Moon that have a minimum radius of 1200 km.
- All meteorite materials are processed.
- The preSolar nebula was grossly homogeneous, but chemically and isotopically zoned in detail, with refractory elements more concentrated in the center, and volatile elements concentrated in outer zones.
- Mineral dust in the preSolar nebula was dominated by pure enstatite and iron metal.

8. Acknowledgment

Special thanks to Janet E. Bowey (University College London) for help with ISO data. We thank our Washington U. colleagues (R. F. Dymek, B. Fegley, B. L. Jolliff, K. Lodders and R. Korotev) and W. Hamilton (Colorado School of Mines) for helpful discussions. Partial support was provided by NSF EAR-0757841 and AST-0908309 funds.

9. References

Amelin, Y., Krot, A.N., Hutcheon, I.D., Ulyanov, A.A. (2002) Lead Isotopic Ages of Chondrules and Calcium-Aluminum-Rich Inclusions. *Science*, Vol. 297 pp. 1678-1683, ISSN: 0036-8075

Armytage, R.M.G., Georg, R.B., Savage, P.S., Williams, H.M., Halliday, A.N. (2011) Silicon isotopes in meteorites and planetary core formation. Geochim. Cosmochim. Acta, vol. 75, 3662-3676

Armitage, P.J. (2011). Dynamics of Protoplanetary Disks. *Annual Review of Astronomy and Astrophysics*, Vol. 49, pp. 195-236, ISSN: 0066-4146

Basu, S., Antia, H. M. (2008). Helioseismology and Solar Abundances. Physics Reports, Vol. 457, No. 5–6, pp. 217-283, ISSN: 0370-1573

Bates, J.B. (1978) Infrared emission spectroscopy. *Fourier Transform IR Spectr.* Vol. 1, pp. 99-142

Benz, W., Slattery W.L., and Cameron A.G.W. (1988) Collisional stripping of Mercury's mantle. *Icarus,* Vol. 74, pp. 516-528, ISSN: 0019-1035

Bernatowicz, T.J., Zinner, E.K. (1997). *Astrophysical implications of the laboratory study of presolar materials*. AIP, New York.

Boss, A.P. (1998). Temperatures in protoplanetary disks. *Ann. Rev. Earth Planet Sci.*, Vol. 26, pp. 53-80, ISSN: 0084-6597

Bowey, J.E. and Hofmeister, A.M. (2005). Overtones and the 5-8 μm spectra of deeply embedded objects. *Monthly Notices of the Royal Astronomical Soc.* Vol. 358, pp. 1383-1393, ISSN: 0035-8711

Brearly, A.J., Jones, R.H., 1998. Chondritic meteorites. *Rev. Mineral.*, Vol. 36, pp. 1-398, ISSN: 1529-6466

Brewster, M.Q. (1992) *Thermal Radiative Transfer and Properties.* John Wiley and Sons, Inc.

Burbine, T.H., Buchanan P.C., Binzel, R.P., Bus S.J., Hiroi T., Hinrichs J.L., Meibom A., and McCoy T.J. (2001) Vesta, vestoids, and the howardite, eucrite, diogenite group: Relationships and the origin of spectral differences. *Meteorites Planet. Sci.*, Vol. 36, pp. 761-781, ISSN: 1086-9379

Burbine, T.H.; Greenwood, R.C.; Buchanan, P.C.; Franchi, I.A., Smith, C.L. (2007). Reflectance spectra of Mesosiderites: Implications for asteroid 4 Vesta. *38th Lunar and Planetary Science Conference*, League City, Texas, USA, 12-16 March 2007

Bus, S.J., Binzel, R.P. (2002). Phase II of the Small Main-Belt Asteroid Spectroscopic Survey. *Icarus*, Vol. 158, pp. 146-177, ISSN: 0019-1035

Basaltic Volcanism Study Project (1981). Basaltic Volcanism on the Terrestrial Planets. Pergamon, New York, ISBN: 0-08-028086-2

Cameron, A.G.W., Fegley, B., Benz, W., & Slattery, W. L. (1988). The strange density of Mercury: theoretical considerations, In: *Mercury*, C. Chapman, C. & Vilas, F. (Eds), pp. 692-708. University of Arizona Press, ISBN 0-8165-1085-7, Tucson, AZ.

Chamberlin, M.A., Sykes, M.V., Tedesco, E.F. (2011). Mid-Infared lightcurve of Vesta. *Icarus*, Vol. 215, (06-2011), pp. 57-61, ISSN: 0019-1035

Christensen, P.R., Bandfield J. L., Hamilton V.E., Howard D.A., Lane M.D., Piatek J.L., Ruff S.W., and Stefanov W.L. (2000) A thermal emission spectral library of rock-forming minerals. *J. Geophys. Res*., Vol. 105, pp. 9735-9739, ISSN: 0885-3401

Clayton, R.N. and Mayeda T.K. (1996) Oxygen isotope studies of achondrites. *Geochim. Cosmochim. Acta*, Vol. 60, pp. 1999-2017, ISSN: 0016-7037

Consolmagno, G.J., Brit, D.T. (2003). Stony meteorite porosities and densities: A review of the data through 2001. *Meteoritics and Planetary Science*, Vol. 38, No. 8, pp. 1161-1180, ISSN: 1086-9379

Criss, R.E., Farquhar, J. (2008). Abundance, Notation, and Fractionation of Light Stable Isotopes. *Reviews in Mineralogy & Geochemistry; Oxygen in the Solar System*, Vol. 68, pp. 15-30, ISSN: 1529-6466

Dotto, E., Muller. T.G., Barucci M.A., Encrenaz Th. Knacke R.F. Lellouch E, Doressoundiram A., Crovisier J., Brucato J.R., Colangeli L., and Mennalla V. (2000). ISO results on bright Main Belt asteroids: PHT-S observations. *Astron. Astrophys.,* Vol. 358, pp. 1133-1141, ISSN: 0004-6361

Drake, M.J. (2001). The eucrite/Vesta story. *Meteor. Planet. Sci.*, Vol. 36, pp. 501-513, ISSN: 1086-9379

Duke, M.B., Silver L.T. (1967). Petrology of eucrites, howardites and mesosiderites. *Geochim. Cosmochim. Acta,* Vol. 58, pp. 3921-3929, ISSN: 0016-7037

Dymek, R.F., Albee A.L., Chodos A.A., and Wasserburg G.J. (1976). Petrography of isotopically-dated clasts in the Kapoeta howardite and petrologic constraints on the evolution of its parent body. *Geochim. Cosmochim. Acta,* Vol. 40, pp. 115-1130, ISSN: 0016-7037

French, B.M. (1998) *Traces of Catastrophe: A Handbook of Shock-Metamorphic Effects in Terrestrial Meteorite Impact Structures.* LPI Contribution No. 954, Lunar and Planetary Institute, Houston.

Franchi, I.A. (2008). Oxygen Isotopes in Asteroidal Materials. *Reviews in Mineralogy & Geochemistry; Oxygen in the Solar System*, Vol. 68, pp. 345-397, ISSN: 1529-6466

Gaffey, M.J. (1976). Spectral reflectance characteristics of the meteorite classes. *J. Geophys. Res.*, Vol. 81, pp. 905-920, ISSN: 0885-3401

Gaffey, M.J. (1997) Surface lithologic heterogeneity of asteroid 4 Vesta. *Icarus,* Vol. 127, pp. 130-157, ISSN: 0019-1035

Gando, A., Gando, Y., Ichimura, K. et al. (2011). Partial radiogenic heat model for Earth revealed by geoneutrino measurements. *Nature Geoscience*, Vol. 4, (09-2011), pp. 647-651, ISSN: 1752-0894

Goldstein, H. (1950). *Classical Mechanics.* Addison-Wesley Publishing Co., Inc., Reading, Massachusetts, ISBN: 0-201-02510-8

Gomes, R., Levinson, H.F., Tsiganis, K., & Morbidelli, A., (2005). Origin of the cataclysmic late heavy bombardment period of the terrestrial planets. *Nature*, Vol. 435, pp. 466-469, ISSN: 0028-0836

Goodrich, C.A.and Bird J.M. (1985). Formation of iron-carbon alloys in basaltic magma at Uivfaq, Disko Island: the role of carbon in mafic magmas. *J. Geology*, Vol. 93, pp. 475-492, ISSN: 0022-1376

Gounelle, M., Spurny, P., Bland, P.A. (2006). The orbit and atmospheric trajectory of the Orgueil meteorite from historical records. *Meteoritics & Planetary Science*, Vol. 41, No. 1, pp. 135-150, ISSN: 1086-9379

Grady, M.M. (2000). *Catalogue of Meteorites*. Cambridge University Press.

Grady, M.M. (2006). The history of research on meteorites from Mars. In: McCall, G.J.H., Bowden, A.J., Howarth, R.J. (Eds.). (2006). *The History of Meteoritics and Key Meteorite Collections: Fireballs, Falls and Finds.* Geological Society, Special Publication 256. 13: 978-1-86239-194-9.

Guan, Y., McKeegan, K.D., MacPherson, G.J. (2000). Oxygen isotopes in calcium-aluminum-rich inclusions from enstatite chondrites: new evidence for a single CAI source in the solar nebula. *Earth and Planetary Science Letters*, Vol. 181, pp. 271-277, ISSN 0012-821X

Heras A.M., Morris P.W., Vandenbussche B., Müller T.G. (2000). Asteroid 4 Vesta as seen with the ISO short wavelength spectrometer. In: *Thermal Emission Spectroscopy and Analysis of Dust, Disks, and Regoliths.* M.L. Sitko, A.L. Sprague, and D.K. Lynch, pp. 205-212, ISBN: 978-1-58381-532-8

Hiroi T., Binzel R.P., Shunshine, J.M., Pieters, C.M., Takeda, H. (1995). Grain sizes and mineral composition of Vesta-like asteroids. *Icarus,* Vol. 115, pp. 374-386, ISSN: 0019-1035

Hofmeister, A.M., Bowey, J.E. (2006). Quantitative IR spectra of hydrosilicates and related minerals. *Monthly Notices Royal Astronomical Society,* Vol. 367, pp. 577-591, ISSN: 0035-8711

Hofmeister, A.M and Criss, R.E. (2005) Earth's heat flux revisited and linked to chemistry. *Tectonophysics,* Vol. 395, pp. 159-177, ISSN: 0040-1951

Hofmeister, A.M and Criss, R.E. (2012). A thermodynamic model for formation of the Solar System via 3-dimensional collapse of the dusty nebula. *Planetary and Space Science*, ISSN 0032-0633 Vol. 62, pp. 111-131

Hofmeister, A.M., Rossman, G.R. (1984). Determination of Fe^{3+} and Fe^{2+} concentrations in feldspar by optical and EPR spectroscopy. *Phys. Chem. Minerals,* Vol. 11, pp. 213-224, ISSN: 0342-1791

Hofmeister, A.M., Keppel E., Speck A.K. (2003). Absorption and reflection spectra of MgO and other diatomic compounds. *Mon. Not. R. Astron. Soc.*, Vol. 345, No. 1, (03-2003), pp. 16-38, ISSN: 0035-8711

Hofmeister, A.M., Wopenka, B, Locock, A., (2004). Spectroscopy and structure of hibonite, grossite, and $CaAl_2O_4$: implications for astronomical environments. *Geochim. Cosmochim. Acta*, Vol. 68, pp. 4485-4503, ISSN: 0016-7037

Javoy, M., 1995. The integral enstatite chondrite model of the earth. *Geophys. Res. Lett.*, Vol. 22, pp. 2219-2222, ISSN: 0094-8276

Kemper, F., Jaeger, C., & Waters L.B.F.M. (2002). Detection of carbonates in dust shells around evolved stars. *Nature,* Vol. 415, pp. 295–297, ISSN: 0028-0836

Kitts K., Lodders, K. (1998). Survey and evaluation of eucrite bulk compositions. *Meteoritics Planet. Sci.,* Vol. 33, pp. 197-213, ISSN: 1086-9379

Lewis, J.S., (1974). The temperature gradient in the solar nebula. *Science*, Vol. 186, pp. 440-43, ISSN: 0036-8075

Lim, L.F., McConnochie, T.H., Bell, J.F., Hayward, T.L. (2005) "Thermal infrared (8-13 μm) spectra of 29 asteroids: the Cornell Mid-Infrared Asteroid Spectroscopy (MIDAS) Survey." *Icarus*, Vol. 173, pp. 385-408, ISSN: 0019-1035

Lodders, K. (1998). A survey of shergottite, nakhlite and chassigny meteorites whole-rock compositions. *Meteoritics Planet. Sci.,* Vol. 33, pp. 183-190, ISSN: 1086-9379.

Lodders, K. (2000). An oxygen isotope mixing model for the accretion and composition of rocky planets. *Space Sci. Rev.*, Vol. 92, pp. 341-354, ISSN: 0038-6308

Lodders, K. (2003). Solar system abundances and condensation temperatures of the elements. *The Astrophysical Journal*, Vol. 591, (06-2003), pp. 1220-1247, ISSN: 0004-637X.

Lodders, K., Fegley, B. (1998). *The Planetary Scientist's Companion*. Oxford, New York.

Love, S.G., Kiel, K. (1995). Recognizing Mercurina meteorites. Meteoritics, Vol. 30, pp269-278, ISSN: 1086-9379.

Low, M.J.D., Coleman, I. (1966). Measurement of the spectral emission of infrared radiation of minerals and rocks using multiple-scan interferometry. *Appl. Opt*. Vol. 5, pp. 1453-1455, ISSN: 1559-128X

Lucey, P.G., Keil K., Whitely, R. (1998). The influence of temperature on the spectra of the A-asteroids and implications for their silicate chemistry. *J. Geophys. Res.*, Vol. 103, pp. 5865-5871, ISSN: 0885-3401

MacPherson, G.J., Simon, S.B., Davis, A.M., Grossman, L., Krot, A.N. (2005). Calcium-Aluminum-rich Inclusions: Major Unanswered Questions. In: Krot, A.N., Scott, E.R.D., Reipurth, B. (2005). *Chondrites and the Protoplanetary Disk ASP Conference Series*, Vol. 341, pp. 225-250, ISSN: 1-58381-208-3

McKeegan, K.D., Leshin, L.A., Russell, S.S., MacPherson, G.J. (1998). Oxygen Isotopic Abundances in Calcium-Aluminium-Rich Inclusions from Ordinary Chondrites: Implications for Nebular Heterogeneity. *Science*, Vol. 280, pp. 414-418 ISSN: 0036-8075

Melosh, H.J., Tonks, W.B. (1993). Swapping Rocks: Ejection and Exchange of Surface Material Among the Terrestrial Planets. *Meteoritics*, Vol. 28, No. 3, vol. 28, (1993), pp. 398, ISSN: 1086-9379

Mittlefehldt, D.W., McCoy, T.J., Goodrich, C.A., Kracher, A. (1998). Non-chondritic meteorites from asteroidal bodies. *Rev. Mineral*, 36, pp. 1-195, 1529-6466

Molini-Velsko, C., Mayeda T.K. and Clayton R.N. (1986) Isotopic composition of silicon in meteorites. *Geochim. Cosmochim. Acta*, Vol. 50, pp. 2719-2726, ISSN: 0016-7037

Molster, F.J., Lim, T.L., Sylvester, R.J., Waters, L.B.F.M. Barlow, M.J., Beintema, D.A., Cohen, M., Cox, P., Schmitt, B., (2001). The complete ISO spectrum of NGC 6302. *Astron. Astrophys.*, Vol. 372, pp. 165–172, ISSN: 0004-6361

Nittler, L.R. and 14 others (2011) The major-element composition of Mercury's surface from MESSENGER X-ray spectrometry. Science, Vol. 333, pp. 1847-1850. ISSN: 0036-8075.

Pepowski, P.N. and 16 others (2011) Radioactive elements on Mercury's surface from MESSENGER: implications for the Planet's formation and evolution. Science, Vol. 333, pp. 1850-1852. ISSN: 0036-8075.

Prinz, M., Weisberg, M.K., Nehru, C.E., MacPherson, G.J., Clayton, R.N., Mayeda, T. (1989). K. Petrologic and Stable Isotope Study of the Kakangari (K-Group) Chondrite: Chondrules, Matrix, CAI's. *Abstracts of the Lunar and Planetary Science Conference*, Vol. 20, p. 870

Ruzicka, A., Snyder G.A., Taylor L.A. (1997). Vesta as the howardite, eucrite and diogenite parent body: implications for the size of a core and for large-scale differentiation. *Meteoritics Planet. Sci.* Vol. 32, pp. 825-840, ISSN: 1086-9379

Shearer, C.K., Fowler G.W., Papike, J.J. (1997). Petrogenic models for magmatism on the eucrite parent body: evidence from orthopyroxene in diogenites. *Meteoritics Planet. Sci.* Vol. 32, p. 877, 1086-9379

Spudis, P.D., Guest, J.E. (1988). Stratigraphy and Geologic History of Mercury. In: *Mercury* The University of Arizona Press, Tuscon, ISBN: 0-8165-1085-7

Surkov, Yu. A., Kirnozov, F.F., Glazov, V.N., Dunchenko, A.G., Tatsy, L.P., Sobornov, O.P. (1987). Uranium, thorium, and potassium in the Venusian rocks at the landing sites of Vega 1 and 2. *J. Geophys. Res.,* Vol. 92, pp. 537-540, ISSN: 0885-3401

Symon, K.R. (1971). *Mechanics*. Addison-Wesley. Reading, Massachusetts.

Taylor, H.P., Duke, M.B., Silver, L.T., Epstein, S. (1965). Oxygen isotope studies of minerals in stony meteorites. *Geochi. Cosmochim. Acta* , Vol. 29, pp. 489-512, ISSN: 0016-7037

Tholen, D.J. (1989). "Asteroid taxonomic classifications". *Asteroids II*. Tucson: University of Arizona Press, ISBN:08165-11233

van Breemen, J.M., Min, M., Chiar, J.E., Waters, L.B.F.M., Kemper, F., Boogert, A.C.A., Cami, J., Decin, L., Knez, C., Sloan, G.C., and Tielens, A.G.G.M., (2011). The 9.7 and 18 mm silicate absoption profiles towards diffuse and molecular cloud lines-of-sight. *Astron. Astrophys*. Vol. 526, in press, ISSN: 0004-6361

Vickery, A.M., Melosh, H.J. (1983). The Origin of SNC Meteorites: An Alternative to Mars. *Icarus*, Vol. 56, pp. 299-318, ISSN: 0019-1035

Wasserburg, G.J., MacDonald G., Hoyle F., and Fowler W.A. (1964). Relative contributions of uranium, thorium and potassium to heat production in the Earth. *Science,* Vol. 143, pp. 465-467, ISSN: 0026-8075

Wetherill, G.W. (1988). Accumulation of Mercury from planetesimals, In: *Mercury*, C. Chapman, C. & Vilas, F. (Eds), pp. 670-691. University of Arizona Press, ISBN 0-8165-1085-7, Tucson, AZ.

Zolensky, M.E. et al., (2006). Mineralogy and petrology of Comet 81P/Wild 2 Nucleus samples. *Science*, Vol. 314, pp. 1735-1739, ISSN: 0036-8075

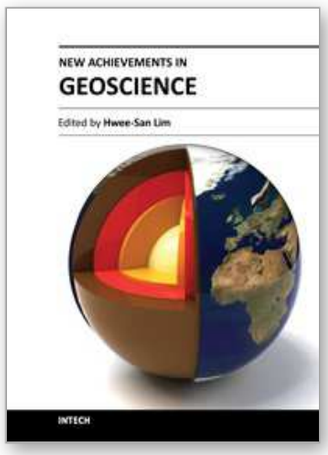

New Achievements in Geoscience

Edited by Dr. Hwee-San Lim

ISBN 978-953-51-0263-2
Hard cover, 212 pages
Publisher InTech
Published online 23, March, 2012
Published in print edition March, 2012

New Achievements in Geoscience is a comprehensive, up-to-date resource for academic researchers in geophysics, environmental science, earth science, natural resource managements and their related support fields. This book attempts to highlight issues dealing with geophysical and earth sciences. It describes the research carried out by world-class scientists in the fields of geoscience. The content of the book includes selected chapters covering seismic interpretation, potential field data interpretation and also several chapters on earth science.

How to reference

In order to correctly reference this scholarly work, feel free to copy and paste the following:

Anne M. Hofmeister and Robert E. Criss (2012). Origin of HED Meteorites from the Spalling of Mercury - Implications for the Formation and Composition of the Inner Planets, New Achievements in Geoscience, Dr. Hwee-San Lim (Ed.), ISBN: 978-953-51-0263-2, InTech, Available from: http://www.intechopen.com/books/new-achievements-in-geoscience/the-case-for-hed-meteorites-originating-in-deep-spalling-of-mercury-implications-for-composition-and

INTECH
open science | open minds

InTech Europe
University Campus STeP Ri
Slavka Krautzeka 83/A
51000 Rijeka, Croatia
Phone: +385 (51) 770 447
Fax: +385 (51) 686 166
www.intechopen.com

InTech China
Unit 405, Office Block, Hotel Equatorial Shanghai
No.65, Yan An Road (West), Shanghai, 200040, China
中国上海市延安西路65号上海国际贵都大饭店办公楼405单元
Phone: +86-21-62489820
Fax: +86-21-62489821

IntechOpen